

# The Rcs regulon in *Proteus mirabilis*: implications for motility, biofilm formation, and virulence

Kristen E. Howery<sup>1</sup> · Katy M. Clemmer<sup>2</sup> · Philip N. Rather<sup>1,2</sup> 

Received: 30 September 2015 / Revised: 5 February 2016 / Accepted: 9 February 2016 / Published online: 2 March 2016  
© Springer-Verlag Berlin Heidelberg (outside the USA) 2016

**Abstract** The overall role of the Rcs phosphorelay in *Proteus mirabilis* is largely unknown. Previous work had demonstrated that the Rcs phosphorelay represses the *flhDC* operon and activates the *minCDE* cell division inhibition system. To identify additional cellular functions regulated by the Rcs phosphorelay, an analysis of RNA-seq data was undertaken. In this report, the results of the RNA-sequencing are discussed with an emphasis on the predicted roles of the Rcs phosphorelay in swarmer cell differentiation, motility, biofilm formation, and virulence. RcsB is shown to activate genes important for differentiation and fimbriae formation, while repressing the expression of genes important for motility and virulence. Additionally, to follow up on the RNA-Seq data, we demonstrate that an *rscB* mutant is deficient in its ability to form biofilm and exhibits enhanced virulence in a *Galleria mellonella* waxworm model. Overall, these results indicate the Rcs regulon in *P. mirabilis* extends beyond flagellar genes to include those involved in biofilm formation and virulence. Furthermore, the information presented in this study may provide clues to additional roles of the Rcs phosphorelay in other members of the *Enterobacteriaceae*.

**Keywords** *Proteus* · Swarming · Rcs phosphorelay

## Introduction

The regulator of colonic acid capsule synthesis (Rcs) phosphorelay is a complex signal transduction system present in many members of the *Enterobacteriaceae*. In the swarming bacterium *Proteus mirabilis*, the Rcs phosphorelay controls swarmer cell differentiation, represses the *flhDC* operon and activates the *minCDE* cell division system (Belas et al. 1998; Liaw et al. 2001; Clemmer and Rather 2008a; Howery et al. 2015). However, our knowledge of the role for the Rcs phosphorelay in other cellular functions in *P. mirabilis* is limited. Because of the importance of *P. mirabilis* as a human pathogen, we sought to identify additional functions for the Rcs phosphorelay in the physiology of this bacterium.

The Rcs phosphorelay was first identified during a screen to find genes necessary for capsular polysaccharide (*cps*) synthesis in *Escherichia coli* (Gottesman et al. 1985). Further studies revealed that it was not just a simple two-component system, but a multifaceted variation known as a phosphorelay. The Rcs phosphorelay comprises a sensor kinase (RcsC) located at the inner membrane, a response regulator (RcsB) (Brill et al. 1988; Stout and Gottesman 1990), and a phosphotransfer protein (RcsD). RcsD, previously known as YojN, mediates the transfer of the phosphate group from RcsC to RcsB (Takeda et al. 2001). An additional protein, RcsA, is an auxiliary protein that assists RcsB binding at sites denoted as RcsAB boxes (Pristovsek et al. 2003; Stout et al. 1991). Finally, the outer membrane lipoprotein RcsF transmits signals induced by membrane stress or other elements to RcsC thereby activating the phosphorelay (Castanie-Cornet et al. 2006; Majdalani et al. 2005; Gervais and Drapeau 1992).

Communicated by M. Kupiec.

**Electronic supplementary material** The online version of this article (doi:10.1007/s00294-016-0579-1) contains supplementary material, which is available to authorized users.

✉ Philip N. Rather  
prather@emory.edu

<sup>1</sup> Department of Microbiology and Immunology, Emory University, 3001 Rollins Research Center, Atlanta, GA, USA

<sup>2</sup> Research Service, Atlanta VA Medical Center, Decatur, GA, USA

In addition to *cps*, other targets for Rcs regulation have been identified in *E. coli*. The cell division septum protein, FtsZ, responsible for Z-ring formation at the future site of cytokinesis is activated by RcsB (Gervais et al. 1992). A related cell division protein, FtsA, which tethers FtsZ to the cell membrane, was also shown to be Rcs regulated (Carballès et al. 1999). OsmC, a reducer of organic hydroperoxides, and two other osmotically induced proteins, encoded by *osmB* and *osmY*, are all Rcs-activated genes (Davalos-Garcia et al. 2001; Hagiwara et al. 2003). RprA, a regulatory RNA also activated by RcsB, affects translation of RpoS, which connects the Rcs phosphorelay to the RpoS regulon (Majdalani et al. 2002). One target in particular, *flhDC*, encoding the regulator for flagellar synthesis, FlhD<sub>4</sub>C<sub>2</sub>, is repressed by the Rcs phosphorelay in *E. coli* (Francez-Charlot et al. 2003) and *Salmonella enterica* (Wang et al. 2007). The relationship between the Rcs phosphorelay and *flhDC* regulation is one that has strong implications for motility and virulence, particularly for organisms that use motility as a means to establish infection.

*Proteus mirabilis* is a highly motile bacterium noted for its ability to change shape from short vegetative rod cells into elongated swarmer cells during a process known as differentiation. Differentiated swarmer cells are 20- to 50-fold longer than their vegetative counterparts and express thousands of flagella (Hoeniger 1965; Belas and Flaherty 1994). Swarmer cells utilize a flagellum-dependent, multicellular form of motility known as swarming which is different from swimming motility. Swimming occurs when a single cell propels itself through liquid or soft agar. Swarming is a multicellular process where a group of cells producing massive amounts of interweaving flagella collectively align and form rafts which facilitate movement across a solid surface (Jones et al. 2004). Differentiation of rod-shaped cells into swarmer cells occurs upon contact with a solid surface. Elements that contribute to this process include O-antigen-mediated cell surface perturbation (Morgenstein et al. 2010), inhibition of flagellar rotation, and cell-to-cell signaling (Rauprich et al. 1996; Fraser and Hughes 1999; Sturgill and Rather 2004; Belas and Sivanasuthi 2005). After a period of migration, swarmer cells undergo consolidation or de-differentiation, which was once thought to be a resting period. However, during consolidation, cells are more metabolically active than swarming cells (Armitage 1981) and a prominent upregulation of genes involved in cell wall synthesis, nutrient uptake, metabolism, and respiration occurs relative to swarming cells (Pearson et al. 2010), indicating the cells are preparing for another period of energy-expensive swarming. The bulls-eye pattern *P. mirabilis* forms on agar plates is due to the oscillation between swarming and consolidation.

At the center of swarmer cell differentiation is the *flhDC* master operon, whose expression is dictated by a myriad of

factors (Belas et al. 1998; Dufour et al. 1998; Liaw et al. 2001; Sturgill and Rather 2004; Stevenson and Rather 2006; Clemmer and Rather 2008a; Morgenstein et al. 2010). The product of *flhDC*, FlhD<sub>4</sub>C<sub>2</sub>, is central to the activation of class II flagellar genes (Furness et al. 1997; Claret and Hughes 2000a), and hyper-flagellation is essential for the formation of swarmer cells (Gygi et al. 1995). Expression of *flhDC* is high during initiation of swarming, but sharp decreases in *flhDC* expression can be observed shortly after differentiation occurs (Furness et al. 1997; Clemmer and Rather 2008a). In addition to strict transcriptional control, the FlhD and FlhC proteins are tightly regulated post-translationally via proteolytic degradation (Claret and Hughes 2000b; Clemmer and Rather 2008b). Modest changes in *flhDC* expression can have dramatic effects on the swarm phenotype. Overexpression of *flhDC* results in a hyperswarming phenotype (Furness et al. 1997), also known as precocious swarming, and *flhDC* mutants do not swarm.

Other mutations that result in hyperswarming include those in the RppAB two-component system (Wang et al. 2008) and the Rcs phosphorelay. It is common in bacteria to employ more than one two-component system to control differentiation (Kovács 2016). The first *rsc* mutations resulting in hyperswarming were in *rscC* and *rscD* (previously *rsbA*) (Belas et al. 1998; Liaw et al. 2001). An *rscB* mutant was later constructed, and it shared the hyperswarming phenotype with other mutants of the Rcs phosphorelay. The hyperswarming phenotype of the *rscB* mutant is likely related to increased levels of *flhDC* observed in this strain (Clemmer and Rather 2008a), and RcsB has been shown to bind to the upstream region of *flhDC* in *E. coli* (Francez-Charlot et al. 2003). In addition to hyperswarming, *rsc* mutants elongate in liquid media, a non-permissive condition for differentiation, suggesting the Rcs phosphorelay influences the expression of genes important for differentiation. Interestingly, *flhDC* overexpression alone does not induce an elongated phenotype in liquid indicating additional *rsc* regulated genes control elongation (Clemmer and Rather 2008a).

Recently, RNA sequencing was performed on an *rscB* mutant in *P. mirabilis* to identify Rcs-regulated genes important for differentiation (Howery et al. 2015). This data set was compiled from three independent RNA-Seq analyses between wild type and an RcsB mutant. GEO accession number GSE76341. However, when re-evaluating these data sets, additional RcsB-regulated genes were identified resulting in 221 genes that were differentially regulated in an *rscB* mutant when a twofold or greater cutoff is employed (Supplemental Table 1). To aid in determining whether RcsB is acting directly or indirectly on genes within its regulon, a bioinformatic approach was used to identify putative RcsB-binding sites. The results of the

RNA-Seq have predicted additional functions that may be controlled by the Rcs regulon in *P. mirabilis*. Specifically, the role of the Rcs regulon in differentiation, motility, self-recognition, adherence, biofilm formation and virulence are discussed. Lastly, to confirm these predictions, we experimentally verify that the Rcs phosphorelay is important for biofilm formation and influences virulence in *P. mirabilis*.

## Materials and methods

### Bacterial growth conditions

Except where indicated, *P. mirabilis* strains were grown in modified Lysogeny (LB) broth (10 g tryptone, 5 g yeast extract, 5 g NaCl/L) at 37 °C with shaking at 250 rpm. Agar was used at 30 g/L in plates to prevent swarming. Antibiotic selections included 35 µg/mL streptomycin.

### Biofilm assays

*Proteus mirabilis* strain HI4320 or the isogenic *rcsB::Str<sup>R</sup>* were grown overnight in LB with appropriate antibiotics at 37 °C without shaking. Cells were equilibrated to the same optical density ( $A_{600}$ ) and a 1:100 dilution of each strain was made in LB only. For the biofilm assays in 96-well polystyrene microtiter plates (Costar®), 150 µL of the diluted cultures were added to 8 wells of the microtiter plate and incubated in a humidified environment at 37 °C for 8 or 24 h. The  $A_{600}$  was determined for each well to measure growth. Biofilms were stained with by adding 15 µL 0.4 % crystal violet to the well and incubating for 15 min. Afterward, stained biofilms were rinsed with deionized water three times, and biofilms were resuspended in 200 µL 33 % acetic acid. Biofilm was quantified by reading each sample at 580 nm and dividing that value by the  $A_{600}$  value for the same sample well. For biofilm assays on catheter, tweezers and scissors were pre-sterilized in 100 % ethanol for 20 min. Siliconized latex catheters (Mentor) were cut into 0.25-in. pieces, flamed briefly, and 5 pieces of catheter were fused per well to the bottom of a 6-well plate (Costar®). 9.5 mL of a 1:100 diluted culture was added in duplicate to the plate containing catheter pieces to submerge them. An LB-only control was used in duplicate. After 8 or 24 h of incubation in a humidified environment, 1 mL of the culture was removed to determine the  $A_{600}$ . If any piece of catheter detached from the bottom of the plate, it was discarded prior to staining. Biofilms were stained by adding 0.85 mL of 0.4 % crystal violet to each well and incubated for 15 min. Liquid was removed from the wells, and catheters were rinsed three times by adding 10 mL deionized water to each well to remove planktonic cells.

After rinsing, catheter pieces were removed and added to individual 1.5 mL microcentrifuge tubes where they were resuspended in 0.9 mL 33 % acetic acid and vortexed for 2 min. Catheter pieces were removed from tubes and each sample tube was read at 580 nm.  $A_{580}$  values were adjusted for each strain by subtracting the average  $A_{580}$  value for catheter incubated in LB only. Biofilm was quantified by dividing the  $A_{580}$  value by the  $A_{600}$  value of the well where catheters were incubated.

### Identification of potential RcsB-binding sites of RcsB-regulated genes

Based on known RcsB-binding sites in *E. coli*, the pattern NNNGANNNCNNN was used as the input for computational microbiology laboratory (CMBL) pattern locator (PATLOC) program (Mrázek and Xie 2006). The search was restricted to intergenic regions within the *P. mirabilis* HI4320 chromosome (NCBI RefSeq NC\_010554.1). Genomic hits returned by PATLOC were compiled using an SAS program to restrict binding sites to RcsB-regulated genes identified using the RNA sequencing data. To confirm location and presence on the direct DNA strand, potential RcsB-binding patterns were input into Nucleotide Basic Local Alignment Search Tool (BLAST) (Altschul et al. 1997) version 2.2.32 adjusted for highly similar (megablast) and short input nucleotide sequences. Potential RcsB-binding sequences located near defined or putative transcriptional regulatory regions were aligned to the consensus *E. coli* RcsAB box, TAAGAATATTCCTA, using an SAS program. Previously identified RcsB-binding sequences in *E. coli* were also aligned. The SAS programs written to compile genomic hits and align binding sequences are available from the authors upon request.

### *Galleria mellonella* killing assays

Cells of wild-type PM7002 or the isogenic *rcsB::Sm* mutant (Clemmer and Rather 2008a) were grown by shaking at 250 rpm in 2.5 mL of LB broth at 37 °C to an optical density ( $A_{600}$ ) of 0.45. A  $10^{-6}$  dilution was prepared in sterile LB and 5 µL representing 10 CFU for each strain was used to inject *G. mellonella* waxworms (200–250 mg each) in the second proleg. The *G. mellonella* worms were incubated at 37 °C in a humidified incubator and were checked at 24 h intervals for killing. Worms were considered dead if they did not move when prodded with a pipette tip and were dark brown or black in color. A total of three independent experiments were conducted representing 28 worms for wild type and 29 worms for the *rcsB* mutant.

## Results

### RcsB-activated genes identified by RNA-Seq

#### Cell division and differentiation

Genes involved in cell division and thus septation have long been hypothesized to play a role in swarmer cell elongation, since the prevention of septation in *E. coli* results in filamentation (de Boer et al. 1989). However, during a previous study to identify genes important for elongation in *P. mirabilis*, only *gidA*, involved in glucose-inhibited cell division, was isolated (Belas et al. 1995). Rcs-activated genes involved in cell division include the Min cell division inhibition system, *ftsZ*, and *ftsA* (Table 1). The Min system is composed of three proteins, MinC, MinD, and MinE, which oscillate from pole to pole during cell division in order to keep FtsZ-mediated Z-ring formation at the cell center (Ward and Lutkenhaus 1985; de Boer et al. 1990). As previously noted, expression of *minC* and *minD* were reduced 3.4- and 6.74-fold, respectively, in the *rcsB* mutant relative to wild type (Table 1 and Howery et al. 2015). FtsZ is the bacterial homolog of tubulin and mediator of the Z-ring (Bi and Lutkenhaus 1991). FtsA, which is structurally related to actin, is the protein that anchors the Z-ring to the site of septation (Pichoff and Lutkenhaus 2005). *ftsZ* expression was reduced 3.33-fold and *ftsA* expression was reduced 2.38-fold in *rcsB* mutant relative to wild type (Table 1). This is consistent with previous studies demonstrating that *ftsZ* and *ftsA* were RcsB activated in *E. coli* (Gervais et al. 1992; Carballès et al. 1999).

An additional Rcs-activated gene important for differentiation was *speB*, where expression was reduced 2.69-fold in the *rcsB* mutant relative to wild type. SpeB functions

as an agmatinase required for the conversion of agmatine to putrescine. Mutations in *speB* result in a delay in the onset of differentiation and shorter migration periods. This swarming defect could be rescued by the addition of extracellular putrescine (Sturgill and Rather 2004).

#### Fimbriae production

*Proteus mirabilis* is known in a clinical setting for its ability to cause catheter-associated urinary tract infections (CAUTIs) which can lead to pyelonephritis, urolithiasis, and cystitis. It is not often found in patients undergoing short-term catheterization (Matsukawa et al. 2005), but can be isolated from the urine of approximately 40 % of patients undergoing long-term catheterization (O'Hara et al. 2000; Jacobsen et al. 2008). The first step in establishing a CAUTI is adherence to a catheter, which *P. mirabilis* readily does (Roberts et al. 1990; Stickler et al. 2006). Fimbriae from other urinary tract pathogens have been implicated in the adherence to catheter material (Mobley et al. 1988; Yakubu et al. 1989). There are 17 putative fimbrial operons in the *P. mirabilis* HI4320 genome (Pearson et al. 2008). The major fimbrial subunits of the mannose-resistant *Proteus*-like (MRP) fimbriae, the *P. mirabilis* fimbriae (PMF), and the uroepithelial cell adhesin fimbriae (UCA) were all identified as Rcs-activated genes. Expression of *mrpA*, *pmfA* and *ucaA* was reduced 68.69-, 63.93-, and 6.97-fold, respectively, in the *rcsB* mutant relative to wild type (Table 1). Additionally, the expression of an *mrpJ* paralog (PMI0261) and a fimbrial adhesin, *mrpH*, paralog (PMI0260) was reduced 28.86- and 12.15-fold (Table 1).

Given the importance of fimbriae to biofilm formation (Jansen et al. 2004; Rocha et al. 2007), the Rcs-mediated activation of certain fimbrial genes in *P. mirabilis*, and the contribution of Rcs to biofilm formation in other bacteria (Ferrières and Clarke 2003; Hinchliffe et al. 2008) biofilm assays were performed using *P. mirabilis* strain HI4320 and an isogenic *rcsB* mutant. After 8 h of incubation in 96-well polystyrene microtiter plates, the *rcsB* mutant was unable to form biofilm (Fig. 1a). After 24 h of incubation, the *rcsB* mutant formed 2.9-fold less biofilm than wild-type cells. The reduction in biofilm formation seen in the *rcsB* mutant at 24 h is unlikely to be the result of increased *flhDC* expression as a wild-type strain that overexpresses *flhDC* on a plasmid (pACYC-*flhDC*) forms the same level of biofilm as cells containing the vector alone (Fig. S1). At 48 h the difference in biofilm formation was not statistically significant, although at this time point the wild-type biofilm had decreased 6.8-fold compared to 24 h. Biofilm reduction after longer periods of incubation is not an uncommon phenomenon and can be seen in other organisms (Jackson et al. 2002; Berne et al. 2010). The reduction over time in wild type is not seen in the *rcsB* mutant, where only a

**Table 1** Rcs-activated genes discussed in this article

Gene	Fold change ( <i>rcsB</i> :: <i>Str<sup>R</sup></i> relative to wild type)
<b>Differentiation</b>	
<i>minD</i>	−6.74
<i>minC</i>	−3.40
<i>ftsZ</i>	−3.33
<i>ftsA</i>	−2.38
<i>speB</i>	−2.69
<b>Fimbriae</b>	
<i>mrpA</i>	−68.69
<i>pmfA</i>	−63.93
PMI0261 ( <i>mrpJ</i> paralog)	−28.86
PMI0260 ( <i>mrpH</i> paralog)	−12.15
<i>ucaA</i>	−6.97

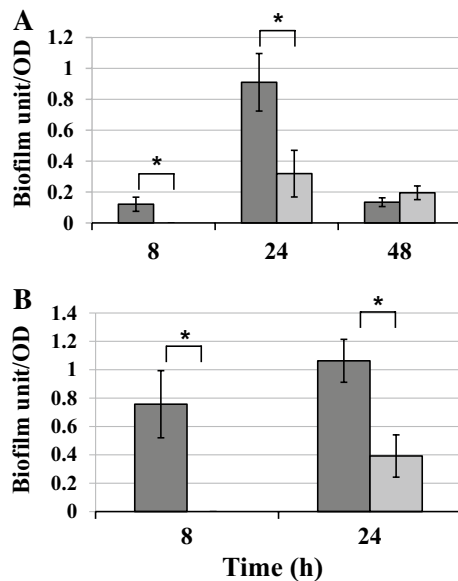


**Fig. 1** An *rcsB* mutant is deficient in biofilm formation. In *Panel a*, *P. mirabilis* strain HI4320 (dark grey bars) or the isogenic *rcsB::Str<sup>R</sup>* (light grey bars) was grown overnight at 37 °C without shaking. Cells were equilibrated to the same optical density ( $A_{600}$ ), diluted, incubated in polystyrene microtiter plates for 8, 24, and 48 h. Biofilm formation was assessed as described in the “Materials and methods”. In *Panel b*, biofilms were formed on 0.25-in. latex catheter pieces for 8 and 24 h. For all experiments, the average of three independent experiments is shown. Error bars represent standard deviations. \* $p$  value < 0.05

0.6-fold reduction in biofilm occurred between 24 and 48 h (Fig. 1a).

To examine the importance of *rcsB* to establishing CAUTIs, additional biofilm assays were performed using siliconized latex catheters. Recapitulating the results of the previous biofilm assays, the *rcsB* mutant did not form detectable biofilm on catheter after 8 h of incubation. After 24 h of incubation, the *rcsB* mutant did form biofilm, but 2.7-fold less than wild type (Fig. 1b). Overall biofilm formation for both strains was higher on catheter material, with the exception of the *rcsB* mutant after 8 h of incubation. In fact, the wild-type strain formed 6.3-fold more biofilm on catheter (Fig. 1b) compared to polystyrene (Fig. 1a) after 8 h of incubation.

## RcsB-repressed genes

### Motility

As the Rcs phosphorelay is a well-characterized repressor of swarming, it was not surprising that a large number of flagellar genes were identified as Rcs-repressed (Table 2). There are 15 proteins that comprise the external structural proteins of the flagellum, and 13 of those were recognized

as Rcs-repressed. They include the proximal rod (FlgB, FlgC, FlgF), the distal rod (FlgG) and rod cap (FlgJ), the hook (FlgE), the hook cap (FlgD), hook-length control protein (FliK), the hook-flagellar junction proteins (FlgK, FlgL), the major flagellar subunit (FlaA) and flagellar cap (FliD), and the anti- $\sigma^{28}$  regulatory protein (FlgM) (Table 2). Secretion of the structural proteins involves seven proteins located within the flagellar basal body, four of which have been identified as Rcs-repressed (FlhB, FliF, FliO, and FliP). All three proteins which comprise the ATPase that drives export of flagellar components (FliI, FliH, and FliJ), the secretion chaperones (FlgN, FliS and FliT), and the alternative sigma factor FliA ( $\sigma^{28}$ ) were all negatively regulated by RcsB (Table 2).

Additional flagellar proteins that were identified as Rcs-repressed are within the basal body and the flagellar motor. They include the flagellar basal body protein FliL, the L-ring protein FlgH, the P-ring proteins FlgA and FlgI, the MS-ring protein FliF, and the C ring proteins (FliG, FliM, and FliN). *motA*, *motB*, and all genes encoding members of the chemosensory (Che) complex with the exception of *cheW*, and two putative methyl-accepting chemotaxis proteins, PMI2808 and PMI2809, were also identified as negatively regulated by RcsB (Table 2).

Important regulators of flagellar synthesis, in addition to *fliA* ( $\sigma^{28}$ ) and *flgM* (anti- $\sigma^{28}$ ), were repressed by RcsB. They include the class I operon for flagellar synthesis, *flhDC*; *umoA* and *umoD* (which were named for the upregulated expression of *flhDC*), and *fliZ*. Finally, *ccmA*, a gene important for cell shape and motility but unrelated to flagella production (Hay et al. 1999) was identified as Rcs-repressed (Table 2).

### Virulence genes

RcsB influences the expression of two well-studied virulence genes, the IgA-degrading protease *zapA* and hemolysin (*hpmBA*). Both *zapA* and *zapB*, encoding a type-1 secretion ATP-binding protein, and *zapD*, encoding a type I secretion outer membrane protein, were found to be Rcs-repressed. The expression of *zapA*, *zapB*, and *zapD* were upregulated 43.44-, 39.44-, and 13.87-fold, respectively, in the *rcsB* mutant relative to wild type (Table 2). Expression of the hemolysin encoding genes, *hpmA* and *hpmB*, was also upregulated 12.51 and 10.41-fold, respectively, in the *rcsB* mutant relative to wild type (Table 2).

The RNA-Seq data suggested that the virulence of an *rcsB* mutant might be enhanced as the *hpmBA* hemolysin and *zapAB* protease genes were overexpressed. To examine this, we used an invertebrate *G. mellonella* waxworm model. In three independent experiments, the average killing at day 1 after infection was 92 % for the *rcsB* mutant versus 34 % for wild-type cells (Fig. 2). At day 2, the

**Table 2** Rcs-repressed genes discussed in this article

Gene	Fold change ( <i>rscB::Str<sup>R</sup></i> relative to wild type)
<b>Virulence factors</b>	
<i>zapA</i>	43.44
<i>zapB</i>	39.44
<i>zapD</i>	13.87
<i>hpmA</i>	12.51
<i>hpmB</i>	10.41
<b>Motility</b>	
<i>fliO</i>	26.61
<i>fliJ</i>	25.48
<i>umoD</i>	21.51
<i>flhB</i>	21.16
<i>ccm</i>	15.90
<i>flhC</i>	15.71
<i>fliP</i>	15.02
<i>fliK</i>	13.28
<i>flgC</i>	13.26
<i>fliZ</i>	13.13
<i>flgF</i>	12.76
<i>fliA</i>	11.51
<i>flgD</i>	11.34
<i>flgK</i>	10.31
<i>flgE</i>	9.47
<i>fliI</i>	9.29
<i>flgJ</i>	9.03
<i>fliH</i>	8.71
<i>fliF</i>	7.99
<i>flgG</i>	7.97
<i>flhD</i>	7.89
<i>fliG</i>	7.33
<i>flgA</i>	7.07
<i>flaD</i>	6.99
<i>fliL</i>	6.52
<i>umoA</i>	5.86
<i>flaA, flgB</i>	5.67
PMI2809 (methyl-accepting chemotaxis protein)	4.93
<i>fliT</i>	4.87
<i>fliM</i>	4.50
<i>fgL</i>	4.15
<i>cheA</i>	4.06
<i>flgN</i>	3.98
<i>motA</i>	3.87
<i>fliN</i>	3.85
<i>fliS</i>	3.84
<i>flgH</i>	3.63
<i>motB</i>	3.59
<i>flgI</i>	3.43
<i>cheZ</i>	2.91

**Table 2** continued

Gene	Fold change ( <i>rscB::Str<sup>R</sup></i> relative to wild type)
PMI2808 (methyl-accepting chemotaxis protein)	2.63
<i>cheB</i>	2.52
<i>flgM</i>	2.45
<i>cheR</i>	2.26
<i>cheY</i>	2.20
<b>Self-recognition</b>	
PMI1332 ( <i>idsF</i> paralog)	35.45
PMI0749 ( <i>tssA</i> )	10.29
PMI0748 ( <i>tssB</i> )	9.01
PMI0747 ( <i>tssC</i> )	7.85
PMI1331 ( <i>idsB</i> paralog)	6.89
PMI0741 ( <i>tssI</i> )	5.90
PMI1118 ( <i>idrB</i> paralog)	5.38
PMI0740 ( <i>tssJ</i> )	4.49
PMI0738 ( <i>tssL</i> )	4.10
PMI0745 ( <i>tssE</i> )	3.90
PMI1117 ( <i>hcp/idrA</i> paralog)	3.89
PMI0742 ( <i>tssH</i> )	3.66
PMI0744 ( <i>tssF</i> )	3.39
PMI0751 ( <i>idrB</i> )	3.21
PMI0750 ( <i>idrA</i> )	3.11
PMI2990 ( <i>idsA</i> )	2.39

percent killing was 96 % for the *rscB* mutant and 53 % for wild type and at day 3, the *rscB* mutant killed 96 % of the worms versus 60 % for wild-type cells.

#### Self-recognition

*Proteus mirabilis* undergoes an interesting phenomenon during swarming where different strains will form boundaries (Dienes lines) between swarming colonies, but swarming colonies of the same strain will merge (Dienes 1946). The ability to distinguish between self and non-self has been well studied in *P. mirabilis* strain BB2000. Two systems, *ids* and *idr*, are important for self-recognition, and their products are exported by a type VI secretion system encoded by *tss* (Gibbs et al. 2008; Wenren et al. 2013, Alteri et al. 2013). The BB2000 homologs of *idsA* (PMI2990), *idrA* (PMI0750), and *idrB* (PMI0751) were all negatively regulated by RcsB (Table 2). PMI1117 (*hcp*) is a paralog of PMI0750, and PMI1118 is a paralog of PMI0751; both were identified as Rcs-repressed. Several homologs of the *tss* system were identified as Rcs-repressed. They include *tssA* (PMI0749), *tssB* (PMI0748), *tssC* (PMI0747), *tssE* (PMI0745), *tssF* (PMI0744), *tssH* (PMI0742), *tssI* (PMI0741), *tssJ* (PMI0740), and *tssL* (PMI0738) (Table 2).

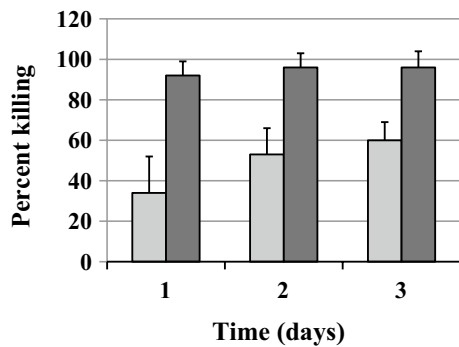


**Fig. 2** An *rcsB* mutant exhibits enhanced virulence in a *Galleria mellonella* waxworm model. Cells of wild-type PM7002 (light grey bars) or the isogenic *rcsB::Str<sup>R</sup>* mutant (dark grey bars) were grown to the same optical density. A  $10^{-6}$  dilution was prepared in sterile LB and was used to inject *G. mellonella* in the second proleg. The *G. mellonella* worms were incubated at 37 °C in a humidified incubator and were checked at 24 h intervals for killing. Worms were considered dead if they did not move when prodded with a pipette tip and were dark brown or black in color. A total of three independent experiments were conducted representing 28 worms for wild type and 29 worms for the *rcsB* mutant. Error bars represent standard deviations

The *idr* and *tss* operons neighbor one another, are positioned divergently, and are separated by a large intergenic region (1899 bp) on the BB2000 chromosome. This organization is mimicked in HI4320 with PMI0250 being separated by an intergenic region of 2396 bp from the BB2000 homolog of *tss*. However, none of the genes downstream of PMI0251 had significant sequence similarity to *idrC*, *idrD*, or *idrE*. Other Rcs-repressed genes, which could be involved in self-recognition include PMI1331, which shares 56 % identity with *IdsB*, and PMI1332, which shares 44 % identity with *IdsF*.

#### Identification of putative RcsB-binding sites upstream of RcsB-regulated genes

As RcsB modulates the expression of known transcriptional regulators such as *flhDC*, *crp*, *rpoN*, and *rpoE*, a bioinformatic approach was used to identify potential RcsB-binding sites upstream of genes identified by the RNA sequencing data. After aligning previously identified RcsB-binding sites (Francez-Charlot et al. 2003; Carballès et al. 1999; Davalos-Garcia et al. 2001), it is clear that the guanine at position 4, the adenine at position 5, and the cytosine at position 10 are the most conserved residues within RcsB-binding sites.

In addition, if point mutations are introduced into the adenine at position 5 or the cytosine at position 10, repression of *flhDC* expression is reduced in *E. coli* (Francez-Charlot et al. 2003). In an *S. enterica* mutant where the Rcs system is constitutively active, a point mutation of the adenine, cytosine, or guanine at position 4 was able to restore

swimming motility in the previously non-motile strain (Wang et al. 2007). These three sites within the RcsAB box are the only residues conserved across strains and multiple genes, both activated and repressed. Therefore, NNNGANNNNNCNNN was used as the input sequence for the Pattern Locator (PATLOC) program (Mrázek and Xie, 2006) against the *P. mirabilis* strain HI4320 genome. When used as the input for PATLOC, 4605 genomic hits were returned. 21.47 % were within pseudogenes, 73.05 % were intergenic, and 5.48 % were partial overlaps. These hits were compiled to be specific for genes identified using the RNA sequencing data. After compilation, the number of hits was reduced to intergenic or partially overlapping regions of 126 genes identified using RNA sequencing. Since PATLOC did not take into account whether the putative site was on the top or bottom strand, each potential sequence was input into BLAST to confirm its location and position. Previously proposed or experimentally identified transcriptional start sites and promoter regions were considered when determining a potential binding site. Thirty-four putative RcsB-binding sites were identified for RcsB-activated genes (Table 3), and 31 putative RcsB-binding sites were identified for RcsB-repressed genes (Table 4). These binding sites were aligned to the original consensus RcsAB box TAAGAATATTCCTA (Wehland and Bernhard 2000) based on the number of shared residues. The consensus RcsAB box was chosen for alignment as it is the originally defined binding sequence for RcsB, though there is divergence amongst identified RcsB-binding sequences, and the RcsB-binding site in *P. mirabilis* is unknown. Shared residues in aligned sequences are shown in red. In addition to putative binding sites, the known RcsA-independent RcsB-binding sites for the promoters of *flhD*, *ftsA*, and *osmC* in *E. coli* are also aligned (Francez-Charlot et al. 2003; Carballès et al. 1999; Davalos-Garcia et al. 2001). The sequence for the RcsA-dependent RcsB-binding site for the *flhD* promoter is also included (Francez-Charlot et al. 2003). Their inclusion in the tables illustrates the divergence of identified RcsB-binding sites from the consensus sequence. The fold-change in gene expression based on the RNA sequencing data and the location of binding site relative to important residues are also included in the table. Unfortunately, for many of the identified genes, no transcriptional start sites or promoters have been mapped and the relevance of the putative binding sites is unclear.

Of the Rcs-activated genes, *cfa* (encoding a cyclopropane fatty acyl phospholipid synthase), *eco* (encoding the protease inhibitor ecotin), and *mrpA* shared the most residues with the RcsB consensus sequence, with 11 out of 14 base pairs aligning with the sequence (Table 3). The location of the RcsB-binding site of *mrpA* is next to the  $-35$  region of a putative  $\sigma^{70}$  promoter, which was identified when the *mrp* operon was first sequenced (Bahrani

**Table 3** Location and putative binding sites of Rcs-activated genes

Gene name	Binding sequence	Location	Count	Fold-change
RcsAB box consensus <sup>a,(104)</sup>	TAAGAATATTCCTA		14	n/a
<i>cfa</i>	TAGGAAAATTCTTA	272 bp upstream of start codon	11	−28.85
<i>eco</i>	TCAGAATAATCCTC	124 bp upstream of start codon	11	−3.69
<i>mrpA</i>	TAGGAATAATCCAA	−40 <sup>(7)</sup> ; +100 <sup>(16)</sup>	11	−68.69
<i>ompA</i>	TAAGATAAGTCATA	289 bp upstream of start codon	10	−52.28
<i>aspA</i>	TAAGAAGGTTCTCA	Overlapping start codon	10	−4.78
PMI3699	TAAGACTTTTCTCA	98 bp upstream of ATG	10	−11.66
<i>dnaK</i>	AATGAATATTCATC	54 bp upstream of ATG	10	−3.54
<i>osmB</i>	CCCGAATATTCTGA	60 bp upstream of start ATG	9	−59.26
<i>osmCp1</i> RcsB box <sup>a</sup>	TCGGAATATCCTGC	−48 <sup>(26)</sup>	8	n/a
PMI0805	TTGGACTAACCATA	29 bp upstream of ATG	8	−2.79
PMI0250	TGAGAGAAATCTGA	177 bp upstream of ATG	8	−3.54
<i>katA</i>	TTAGATTTTCAAT	182 bp upstream of ATG	8	−4.44
<i>crp</i>	TCCGAATTCTCAGG	95 bp upstream of ATG	7	−2.40
PMI3443	TATGAACAACCGAT	83 bp upstream GTG	7	−3.43
<i>pepD</i>	TTTGAGCGTTCAAA	264 bp upstream of GTG	7	−2.06
PMI2837	TATGATAAATCAAT	30 bp upstream of ATG	7	−11.33
<i>frdA</i>	ACCGAGAATTCTTG	247 bp upstream of ATG	7	−4.03
<i>rpoB</i>	ATGGAAAATTCTAT	100 bp upstream of ATG	7	−2.22
<i>ftsAp1</i> RcsB box <sup>a</sup>	GAAGATTCATCTGG	−50 <sup>(18)</sup>	7	n/a
<i>ftsA</i>	GCCGAATTTTCAGT	396 bp upstream of ATG	7	−2.38
PMI0044	AGCGAAAATTCAAT	287 bp upstream of ATG	7	−6.70
PMI2772	AATGAGTAATCACT	2 bp upstream of ATG	7	−3.11
<i>ribF</i>	AGTGAGTAATCGTT	151 bp upstream of ATG	7	−4.41
<i>udp</i>	ATTGAGGAGTCCGA	2 bp upstream of ATG	7	−3.48
<i>nrdD</i>	AATGAGCAATCATT	257 bp upstream of GTG	7	−18.11
<i>rraA</i>	CTGGACTTTCCTGA	20 bp upstream of ATG	6	−2.50
<i>uspA</i>	ACCGATTAATCAGC	19 bp upstream of ATG	6	−4.20
<i>pgk</i>	TGTGATAATGCGCG	52 bp upstream of ATG	6	−2.44
<i>poxB</i>	AGAGATTACCCACT	24 bp upstream ATG	6	−6.87
PMI1017	AGCGATTTGGCTTA	113 bp upstream of ATG	6	−4.36
<i>tpx</i>	AGCGAGTTAACTTA	188 bp upstream of ATG	6	−2.44
<i>rpoN</i>	GAGGATCCATCGCA	6 bp upstream of ATG	6	−3.11
PMI0657	TTTGATAAGCCTAT	204 bp upstream of start codon	5	−4.44
<i>rpoE</i>	CGGGAGAGTCCATC	2 bp upstream of ATG	5	−3.04
PMI1454	TCTGATTTAACGCT	49 bp upstream of ATG	5	−4.59
PMI1199	TGTGATAGATCACT	50 bp upstream of ATG	5	−3.73
<i>speB</i>	GTTGATACATCACT	60 bp upstream of ATG	4	−2.70

Superscript numbers represent the number of the citation where relevant sites were previously defined

<sup>a</sup> Denotes previously reported RcsB-binding sequence

and Mobley 1994). The *mrp* transcriptional start site and another  $\sigma^{70}$  promoter were recently identified within the invertible repeat region when the phase variable *mrp* operon is in ON phase (Bode et al. 2015). This places the putative binding site 100 base pairs downstream of the transcriptional start site. Regulatory elements of *cfa* or *eco* have not been identified.

Genes directly regulated by RcsB in other organisms, which were identified in *P. mirabilis* using RNA sequencing include *osmB* and *ftsA*. Their putative binding sites are located 60 and 396 base pairs, respectively, upstream of their start codons. The *osmB* sequences shares 9 out of 14 identities with the consensus RcsAB box and shares 10 out of 14 residues with the *osmCp1* RcsB-binding sequence



**Table 4** Location and putative binding sites of Rcs-repressed genes

Gene name	Binding sequence	Location	Count	Fold-change
RcsAB box consensus <sup>a,(104)</sup>	TAAGAATATTCCTA		14	n/a
<i>flhD</i>	TAGGATTATTCTTA	+3 <sup>(38, 24, 16)</sup>	11	7.90
<i>flhD3</i> RcsB box <sup>a</sup>	TAGGAATTCTCCGA	+5 <sup>(35)</sup>	10	n/a
<i>flhD</i> RcsAB box <sup>a</sup>	TAGGAAAAATCTTA	+5 <sup>(35)</sup>	10	n/a
PMI1359	TTAGAATAATCAAA	213 bp upstream of ATG	10	31.60
PMI1075	AATGAATTTTCCTT	116 bp upstream of ATG	10	10.92
PMI1540	TAAGATTTCTCTTT	250 bp upstream of GTG	9	7.47
<i>fliA</i>	TATGACCCATCTTA	178 bp upstream of ATG	8	11.51
<i>ddg</i>	TAGGAAAAAGCCGT	135 bp upstream of GTG	8	29.34
<i>flaA</i>	AATGAATAGGCAAA	26 bp downstream of $\sigma$ -28 promoter <sup>(9)</sup>	8	5.69
PMI3378	AGAGATAATTCTGA	28 bp upstream of ATG	8	5.21
<i>hcp</i>	AGTGACTTATCCTA	167 bp upstream of ATG	8	3.89
PMI0750	AGTGACTTATCCTA	167 bp upstream of ATG	8	3.11
PMI2990	AGTGACTTATCCTA	167 bp upstream of ATG	8	2.39
<i>hpmB</i>	<u>GTAGATAACGCTTA</u>	Overlapping $\sigma$ -28 promoter (underlined) <sup>(36)</sup>	7	10.41
PMI1438	AGAGATTAACCTAA	37 bp upstream of ATG	7	13.36
PMI0720	ATAGAAATTACTTT	280 bp upstream of ATG	7	3.46
<i>coaE</i>	GAAGATTTAGCCAC	160 bp upstream of ATG	7	3.98
<i>flgA</i>	ACAGAATAAACGCT	86 bp upstream of +1 <sup>(23)</sup>	7	7.07
<i>flgB</i>	ATAGAAGATGCTCG	Overlapping start codon; 42 bp downstream of +1 <sup>(23)</sup>	7	5.67
<i>flhB</i>	<u>AGAGACATTTTCATT</u>	Overlapping +1 (underlined) <sup>(21)</sup>	7	21.16
<i>rpmE</i>	TATGATCCGCCCC	98 bp upstream of ATG	6	2.76
<i>flgM</i>	AAGGATTTTCCTAT	Overlapping start codon (underlined)	6	2.46
PMI2809	TCAGACAGCACTTT	283 bp upstream of ATG	6	4.94
PMI1245	AATGATATAGCCTT	47 bp upstream of ATG	6	234.48
<i>flaD</i>	<u>TCCGATAACGCTGT</u>	Overlapping $\sigma$ -28 promoter (underlined) <sup>(9)</sup>	5	6.99
<i>fliF</i>	<u>AATGAGACACCTGA</u>	Overlapping putative $\sigma$ -28 promoter (underlined)	5	7.99
<i>fliL</i>	ACAGAAATAGCGGG	81 bp upstream of ATG	5	6.52
PMI2121	CTTGAAAAAACACT	33 bp upstream of ATG	5	17.38
PMI2810	TGTGATTTAGCGAT	122 bp upstream of ATG	5	3.17
PMI3393	AAAGATATAACGAC	31 bp upstream of ATG	5	17.06
PMI1628	GGGGACCCATCAGC	31 bp upstream of ATG	4	14.20
<i>motA</i>	<u>AGGGATATCGCGTG</u>	Overlapping start codon (underlined)	4	3.87
PMI2808	GTGGAGCTCCCACT	34 bp upstream of ATG	3	11.53

Superscript numbers represent the number of the citation where relevant sites were previously defined

<sup>a</sup> Denotes previously reported RcsB-binding sequence

(Davalos-Garcia et al. 2001). The *ftsA* binding sequence shares seven residues with the consensus sequence, but nine with the *ftsA1p* binding site of *E. coli*. The putative RcsB-binding site and the *ftsA1p* binding site are found in similar locations: at the center of *ftsQ* (Carballès et al. 1999).

Of the Rcs-repressed genes, the identified RcsB-binding site of *flhD* shared 11 out of 14 residues with the RcsAB consensus sequence and the RcsAB binding site of *flhD* in *E. coli* (Francez-Charlot et al. 2003). It shared nine residues with the RcsA-independent binding site *flhD3p* described

in the same manuscript (Table 4). The putative *flhD* binding site is located two base pairs upstream of the mapped transcriptional start site (Furness et al. 1997; Clemmer and Rather 2008a; Bode et al. 2015). The putative RcsB-binding sites of PMI1359, which encodes a putative attachment invasion outer membrane protein, and PMI1075, a hypothetical protein with a domain of unknown function (DUF1795) aligned 10 of 14 residues with the RcsAB box. Many of the motility-associated genes have putative RcsB-binding sites overlapping their promoters (*hpmB*, *flaD*, *fliF*), start codons (*flgB*, *flgM*, *motA*) or transcriptional

start sites (*flhB*). Additionally, the genes encoding self-recognition proteins PMI1117 (*hcplidrA* homolog), PMI0750 (*idrA* paralog), and PMI2990 (*idsA* homolog) all share the same putative RcsB-binding sequence in the same location (Table 4).

## Discussion

The importance of the Rcs phosphorelay in *P. mirabilis* has long been associated with the control of swarming via the negative regulation of *flhDC*. Through RNA sequencing, we have shown that the impact of Rcs on gene expression extends far beyond the inhibition of swarming-related genes. RcsB is not just a repressor of *flhDC*, but a repressor of many genes essential for motility, including flagella, chemotactic proteins, and positive regulators of motility. In addition, it represses the expression of virulence factors associated with swarmer cells, including *zapA* and hemolysin, and genes important for self-recognition. In contrast, RcsB is an activator of genes important for swarmer cell differentiation, including *minCDE* and *speB*, and also fimbrial genes, which are important for adherence and biofilm formation. This work will pave the way for future studies to identify the specific RcsB-regulated genes that carry out the above functions. In addition, the role of downstream transcriptional regulators in the overall RcsB regulon can be assessed.

As expected, RcsB was shown to negatively regulate the expression of flagellar structural genes and known activators of flagellar synthesis. The negative effect of RcsB on motility is seen in a myriad of bacterial species (Takeda et al. 2001; Wang et al. 2007; Hinchliffe et al. 2008). A putative RcsB-binding site was identified for the master operon for flagellar synthesis, *flhDC* (Table 4); this site shares high sequence homology to the RcsAB consensus binding site and is located in a similar region as the RcsB-binding site of *flhD* in *E. coli*. RcsB-mediated regulation of *flg*, *fli*, or *flhBA* operons could be indirect, as FlhD<sub>4</sub>C<sub>2</sub> has been shown to bind directly to these operons in *E. coli* (Claret and Hughes 2002). FliA, which also has a predicted RcsB-binding motif (Table 4) has also been shown to bind directly upstream of *motAB-cheAW*, predicted methyl-accepting chemotaxis proteins, and the *E. coli* homolog of *flaA* (Fitzgerald et al. 2014).

The RNA sequencing data have revealed new processes controlled by RcsB. First, the expression of self-recognition systems involved in the territoriality of swarmer cells (*ids*, *idr*, *tss*) were repressed by RcsB. Since self-recognition systems are primarily observed under swarming permissive conditions, the increased expression of these genes when swarming has initiated would make biological sense. Second, expression of the *speB* gene, encoding agmatinase,

was reduced 2.69-fold in the RcsB mutant (Table 1). SpeB is required for the production of putrescine and *speB* mutants exhibit both delay in the onset of differentiation and a crippled swarming phenotype.

RcsB also regulated expression of the major fimbrial subunits of the uroepithelial cell adhesion (UCA), the *P. mirabilis* fimbriae (PMF), and the mannose-resistant *Proteus*-like (M/RP) fimbriae, which were highly down-regulated in the *rscB* mutant relative to wild type. Additional genes within each of these fimbrial operons were identified as Rcs-regulated. However, due to low levels of transcript reads, the *p* values for each gene were too high to be deemed significant, and they were not included. RcsB has been shown to directly bind to the promoter region of the *mat* fimbriae and activate its expression in the *E. coli* (Lehti et al. 2012). It also activates the transcription of the *fim* operon in *E. coli* by influencing the orientation of the *fimAp* invertible repeat (Schwan et al. 2007). In addition, *fim* genes are positively regulated by RcsB in *S. enterica* serovar typhimurium (Wang et al. 2007). Identification of major fimbrial subunits in *P. mirabilis* as RcsB regulated is important, as all three systems have been implicated in virulence. Though the contribution of *P. mirabilis* fimbriae to catheter adherence has not been well-characterized, their importance to the establishment of urinary tract infections has been recognized. Mutations in *ucaA* lead to impaired adhesion to uroepithelial cells and in the ability to colonize the kidneys of mice (Pellegrino et al. 2013). Mutants of *pmfA* have been shown to be deficient in bladder colonization in a mouse model of ascending urinary tract infection, but able to colonize the kidneys (Massad et al. 1994). Another study showed that *pmfA* mutants were unable to colonize the bladder and the kidneys (Zunino et al. 2003). The ability of a *pmfA* mutant to adhere to uroepithelial cells also differed between these two reports. The differences seen between these two studies could be due to the route of infection, different strains of mice, uroepithelial cells, and *P. mirabilis*. Mutants of *mrpA* reduce *P. mirabilis* colonization of the bladder, kidneys, and urine of mice (Bahrani et al. 1994; Zunino et al. 2001). M/RP fimbriae are also important for adherence to uroepithelial cells (Zunino et al. 2001) and biofilm formation in *P. mirabilis* (Jansen et al. 2004).

*mrpJ* has 14 paralogues in *P. mirabilis* strain HI4320, and many of them repress motility (Pearson and Mobley 2008). MrpJ itself has been shown to directly repress *flhDC* expression (Li et al. 2001; Bode et al. 2015). One *mrpJ* paralog, PMI0261, was highly repressed in the *rscB* mutant based on our RNA sequencing data. The neighboring *mrpH* paralog, PMI0260, was also significantly down-regulated in the *rscB* relative to wild type. Expression of the *mrpA* paralog of this operon (PMI0254) was also reduced in the *rscB* mutant relative to wild type as well as other members

of the paralog operon. Their exclusion is due to a high  $p$  value which resulted from low transcript levels. Why the two terminal genes of this operon produced more read transcript relative to the rest of operon members is unknown. An internal promoter could exist or perhaps more levels of *mrpH* and *mrpJ* are required to initiate transcription of the operon, as *mrpJ* binds and activates expression of *mrpA* (Bode et al. 2015), and assembly of the fimbriae, which *mrpH* is essential for (Li et al. 1999). However, PMI0256, encoding a fimbrial chaperone *mrpD* paralog, is a pseudogene due to the presence of a stop codon. This likely renders this *mrp* paralog non-functional. Overexpression of PMI0261 has been shown to reduce motility in *P. mirabilis* (Pearson and Mobley 2008) in the same manner as *mrpJ*, illustrating its function in counteracting motility is intact. This negative impact fimbrial activators have on motility makes biological sense as motile bacteria would not want to express adherence factors and vice versa.

The formation of biofilms was strongly impacted by the *rcsB* mutation. Two different biofilm assays were performed, one using polystyrene (Fig. 1a) and the other using catheter sections as biofilm substrates (Fig. 1b). With polystyrene as the substrate, the *rcsB* mutant formed no detectable biofilm after 8 h of incubation, formed 2.9-fold less biofilm than wild type after 24 h, and formed similar amounts of biofilm as wild type after 48 h of incubation. The wild-type strain exhibited a large reduction in biofilm formation between 24 and 48 h of incubation which was not as exaggerated in the *rcsB* mutant (Fig. 1a). The inability of the *rcsB* mutant to form biofilm was recapitulated when assays were performed on catheters. Again, it did not form detectable biofilm after 8 h of incubation, and formed 2.7-fold less biofilm than wild type after 24 h of incubation (Fig. 1b). The inability of the *rcsB* mutant to form biofilm initially may be due to the down-regulation of adherence factors, such as the major fimbrial subunits (*ucaA*, *pmfA*, and *mrpA*). Rcs mutants of *Yersinia pseudotuberculosis* are deficient in their ability to adhere to HEp-2 cells and form biofilm on abiotic surfaces; fimbrial proteins are a part of its RcsB regulon (Hinchliffe et al. 2008). Our RNA-seq data also showed that outer membrane protein A (*ompA*) is highly repressed in the *rcsB* mutant; it has been shown to bind abiotic surfaces, which could contribute to initial adherence (Lower et al. 2005). However, other factors are likely mediating adherence as the *rcsB* mutant does form biofilm after 24 h of incubation. Like wild-type cells, biofilm production of the *rcsB* mutant decreases after 48 h. Overall these data, combined with a previous report that a *P. mirabilis rcsD* mutant is deficient in biofilm production (Liaw et al. 2004), reiterate the contribution of the Rcs phosphorelay to biofilm formation in *P. mirabilis*. These results also suggest a preference for *P. mirabilis* to form biofilm on catheter versus polystyrene, a medically relevant

finding, as the wild-type strain formed 6.8-fold more biofilm on catheter versus polystyrene after 8 h of incubation.

The virulence genes *zapAB* and *hpmBA* were strongly upregulated in the *rcsB* mutant; both have increased expression in swarming bacteria (Walker et al. 1999; Fraser et al. 2002). ZapA is a metalloprotease, which cleaves immunoglobulins (Senior et al. 1991), host cytoskeletal and matrix proteins, complement (C1q and C3), and antimicrobial peptides (human beta-defensin 1 and LL-37) (Belas et al. 2004). It is important for the colonization and subsequent infection of the urinary tract (Phan et al. 2008). HpmA functions as a hemolysin (Mobley et al. 1991; Chippendale et al. 1994) and induces cytotoxicity (Swihart and Welch 1990). Virulence proteins are RcsB regulated in *Y. pseudotuberculosis*, and genes within the *Salmonella enterica* serovar typhimurium SP-2 pathogenicity island are highly repressed by RcsB (Hinchliffe et al. 2008; Wang et al. 2007). Additionally, a mutant of *S. enterica* with a constitutively activated Rcs system is attenuated in virulence within a mouse (Garcia-Calderon et al. 2005). Based on these studies and our RNA-seq data, it was hypothesized that RcsB would regulate virulence in *P. mirabilis*. This was tested using a *Galleria mellonella* waxworm model. It should be noted that this model has not been previously used in *P. mirabilis*, although it has been used in other bacteria, where a good correlation has been observed with mammalian virulence (Jander et al. 2000; Seed and Dennis 2008; Murherjee et al. 2010; Fedhila et al. 2010; Ramarao et al. 2012). Moreover, the relevance of this model to a mouse model of urinary tract infection is unknown, but this model was only intended to measure general differences in virulence. One day after inoculation, the *rcsB* mutant had killed 94 % of worms versus 37 % for wild-type HI4320. By day three, the *rcsB* mutant had killed 96 % of worms versus 60 % of wild type.

A putative RcsB-binding sequence lies upstream of the *hpmBA* operon, but not upstream of the *zap* operon. RcsB has been shown to directly bind to the promoter region of the hemolysin homolog (*shlBA*) in *Serratia marcescens* (Di Venanzio et al. 2014), and our putative RcsB-binding site does overlap the  $\sigma^{28}$  promoter identified by Fraser et al. However, a limitation exists in our identification of putative RcsB-binding sites. By using NNNGANNNNCN as the input, many genomic hits were returned to due the sequence being nonspecific. The input sequence retaining only 3 of 14 base pairs is due to the variability in known RcsB-binding sites. The original RcsAB Box was defined as TaAGaataTCctA, with capital letters being the most conserved residues (Wehland and Bernhard 2000). This binding site was defined based on the RcsA-dependent RcsB-binding site of 12 promoters that were RcsAB regulated. It does not take into account sequence of RcsA-independent RcsB-binding sites of multiple genes. Presently, the RcsB-binding site in *P. mirabilis* is unknown.

The role of the Rcs phosphorelay in establishing CAU-TIs has not been determined, but likely depends on whether the swarmer cell or swimmer cell is more important for colonization of the urinary tract. Conflicting data exist concerning this topic. Studies have shown that differentiated swarmer cells invade uroepithelial cells more efficiently than vegetative cells (Allison et al. 1992), and non-swarming mutants are unable to establish ascending urinary tract infections or kill mice (Allison et al. 1994; Mobley et al. 1996). Other studies have shown swimmer cells, not swarmer cells, are the dominant cell morphology in a mouse model of ascending urinary tract infection (Jansen et al. 2003) and non-flagellated *P. mirabilis* were isolated from a human infection (Zunino et al. 1994). Corroborating these studies is one that showed flagellar genes were down-regulated during the early stages of ascending urinary tract infection. Fimbrial genes, associated with swimmer cells, were upregulated during early infection (Pearson et al. 2011). Perhaps swarmer cells are needed to establish infection, as *P. mirabilis* readily moves across catheters (Sabbuba et al. 2002), but the antigenic potential due to flagellar components and cell length leads to immune recognition. This leads to the selection of swimmer cells in the urinary tract. The upregulation of fimbriae during colonization offers another set of antigens subject to immune recognition. To counteract this, *P. mirabilis* may differentiate into swarmer cells during later stages of infection, consistent with a previous study where fimbrial gene expression decreased while the expression of some flagellar genes increased during the later stages of a mouse ascending urinary tract infection (Pearson et al. 2011). The possibility of cycling differentiation and consolidation during infection reiterates the origin of the name *Proteus*, named for a god who changed shape to avoid capture and questioning. The interplay of the Rcs phosphorelay, together with additional important genetic factors contributes to this elusive change in cell morphology and affects motility, biofilm formation, and virulence in *P. mirabilis*.

**Acknowledgments** This work was supported by a Merit Review award 11OIBX001725 and by a Research Career Scientist award to P.N.R., both from the Department of Veterans Affairs. K.H. was supported by the Burroughs Wellcome Fund's Molecules to Mankind program. The authors thank Lewis Jordan, PhD, for aid in the bioinformatic identification of RcsB-binding sites.

## References

- Allison C, Coleman N, Jones PL, Hughes C (1992) Ability of *Proteus mirabilis* to invade human urothelial cells is coupled to motility and swarming differentiation. *Infect Immun* 60:4740–4746
- Allison C, Emody L, Coleman N, Hughes C (1994) The role of swarm cell differentiation and multicellular migration in the uropathogenicity of *Proteus mirabilis*. *J Infect Dis* 169:1155–1158
- Alteri CJ, Himpf SD, Pickens SR, Lindner JR, Zora JS, Miller JE, Arno PD, Straight SW, Mobley HLT (2013) Multicellular bacteria deploy the type VI secretion system to preemptively strike neighboring cells. *PLoS Pathog* 9(9):e1003608
- Altschul SF, Madden TL, Schäffer AA, Zhang J, Zhang Z, Miller W, Lipman DJ (1997) Gapped BLAST and PSI-BLAST: a new generation of protein database search programs. *Nucleic Acids Res* 25:3389–3402
- Armitage JP (1981) Changes in metabolic activity of *Proteus mirabilis* during swarming. *J Gen Microbiol* 125:445–450
- Bahrani FK, Mobley HLT (1994) *Proteus mirabilis* MR/P fimbrial operon: genetic organization, nucleotide sequence, and conditions for expression. *J Bacteriol* 176(11):3412–3419
- Bahrani FK, Massad G, Lockett CV, Johnson DE, Russell RG, Warren JW, Mobley HLT (1994) Construction of an MR/P fimbrial mutant of *Proteus mirabilis* role in virulence in a mouse model of ascending urinary tract infection. *Infect Immun* 176:3412–3419
- Belas R, Flaherty D (1994) Sequence and genetic analysis of multiple flagellin-encoding genes from *Proteus mirabilis*. *Gene* 128:33–41
- Belas R, Suvanasuthi R (2005) The Ability of *Proteus mirabilis* to sense surfaces and regulate virulence gene expression involves FliL, a flagellar basal body protein. *J Bacteriol* 187(19):6789–6803
- Belas R, Goldman M, Ashliman K (1995) Genetic analysis of *Proteus mirabilis* mutants defective in swarmer cell elongation. *J Bacteriol* 177:823–828
- Belas R, Schneider R, Melch M (1998) Characterization of *Proteus mirabilis* precocious swarming mutants: identification of *rsbA*, encoding a regulator of swarming behavior. *J Bacteriol* 180(23):6126–6139
- Belas R, Manos J, Suvanasuthi R (2004) *Proteus mirabilis* ZapA metalloprotease degrades a broad spectrum of substrates, including antimicrobial peptides. *Infect Immun* 72(9):5159–5167
- Berne C, Kysela DT, Brun YV (2010) A bacterial extracellular DNA inhibits settling of motile progeny cells within a biofilm. *Mol Microbiol* 77(4):815–829
- Bi EF, Lutkenhaus J (1991) FtsZ ring structure associated with division in *Escherichia coli*. *Nature* 354:161–164
- Bode NJ, Debnath I, Kuan L, Schulfer A, Ty M, Pearson MM (2015) Transcriptional analysis of the MrpJ network: modulation of diverse virulence-associated genes and direct regulation of *mrp* fimbrial and *flhDC* flagellar operons in *Proteus mirabilis*. *Infect Immun* 83(6):2542–2556
- Brill JA, Quinlan-Walsh C, Gottesman S (1988) Fine-structure mapping and identification of two regulators of capsule synthesis in *Escherichia coli* K-12. *J Bacteriol* 170:2599–2611
- Carballés F, Bertrand C, Bouche JP, Cam K (1999) Regulation of *Escherichia coli* cell division genes *ftsA* and *ftsZ* by the two-component system *rscC-rscB*. *Mol Microbiol* 34(3):442–548
- Castanie-Cornet MP, Cam K, Jacq A (2006) RcsF is an outer membrane lipoprotein involved in the RcsCDB phosphorelay signaling pathway in *Escherichia coli*. *J Bacteriol* 188:4264–4270
- Chippendale GR, Warren JW, Trifillis AL, Mobley HLT (1994) Internalization of *Proteus mirabilis* by human renal epithelial cells. *Infect Immun* 62(8):3115–3121
- Claret L, Hughes C (2000a) Functions of the subunits of FlhD<sub>2</sub>C<sub>2</sub> transcriptional master regulator of bacterial flagellum biogenesis and swarming. *J Mol Biol* 303:467–478
- Claret L, Hughes C (2000b) Rapid turnover of FlhD and FlhC, the flagellar regulon transcriptional activator proteins, during *Proteus* swarming. *J Bacteriol* 182(3):833–836
- Claret L, Hughes C (2002) Interaction of the atypical prokaryotic transcription activator FlhD<sub>2</sub>C<sub>2</sub> with early promoters of the flagellar gene hierarchy. *J Mol Biol* 321(2):185–199

- Clemmer KM, Rather PN (2008a) Regulation of *flhDC* expression in *Proteus mirabilis*. Res Microbiol 158:295–302
- Clemmer KM, Rather PN (2008b) The Lon protease regulates swarming motility and virulence gene expression in *Proteus mirabilis*. J Med Microbiol 57(8):931–937
- Davalos-Garcia M, Conter A, Toesca I, Gutierrez C, Cam K (2001) Regulation of *osmC* gene expression by the two component system *rcsB-rcsC* in *Escherichia coli*. J Bacteriol 183:5870–5876
- de Boer PA, Crossley RE, Rothfield LI (1989) A division inhibitor and a topological specificity factor coded for by the minicell locus determine proper placement of the division septum in *E. coli*. Cell 56:641–649
- de Boer PA, Crossley RE, Rothfield LI (1990) Central role for the *Escherichia coli minC* gene product in two different cell division-inhibition systems. Proc Natl Acad Sci USA 87:1129–1133
- Di Venanzio G, Stepanenko TM, Garcia Vescovi E (2014) *Serratia marcescens* Sh1A pre-forming toxin is responsible for early induction of autophagy in host cells and is transcriptionally regulated by RcsB. Infect Immun 82(9):3542–3554
- Dienes L (1946) Reproductive processes in *Proteus* cultures. Proc Soc Exp Biol Med 63:265–270
- Dufour A, Furness RB, Hughes C (1998) Novel genes that upregulate the *Proteus mirabilis flhDC* master operon controlling flagellar biogenesis and swarming. Mol Microbiol 29:741–751
- Fedhila S, Buisson C, Dussurgent C, Serror P, Glomsk IJ, Leihl P, Lereclus C, Nielson-LeRoux C (2010) Comparative analysis of the virulence of invertebrate and mammalian pathogenic bacteria in the oral insect infection model *Galleria mellonella*. J Invertebr Pathol 103:24–29
- Ferrières L, Clarke DJ (2003) The RcsC sensor kinase is required for normal biofilm formation in *Escherichia coli* K-12 and controls the expression of a regulon in response to growth on a solid surface. Mol Microbiol 50:1665–1682
- Fitzgerald DM, Bonocora RP, Wade JT (2014) Comprehensive mapping of the *Escherichia coli* flagellar regulatory network. PLoS Genet 10(10):e1004649
- Francez-Charlot A, Laugel B, VanGemert A, Dubarry N, WiorowskiF Castanié-Cornet MP, Gutierrez C, Cam K (2003) RcsCDB His-Asp phosphorelay system negatively regulates the *flhDC* operon in *Escherichia coli*. Mol Microbiol 49:823–832
- Fraser GM, Hughes C (1999) Swarming motility. Curr Opin Microbiol 2:630–635
- Fraser GM, Claret L, Furness R, Gupta S, Hughes C (2002) Swarming-coupled expression of the *Proteus mirabilis hpmBA* haemolysin operon. Microbiol. 148(7):2191–2201
- Furness RB, Fraser GM, Hay NA, Hughes C (1997) Negative feedback from a *Proteus* Class II flagellum export defect to the *flhDC* master operon controlling cell division and flagellum assembly. J Bacteriol 179:5585–5588
- Garcia-Calderon CB, Garcia-Quintanilla M, Casades J, Ramos-Morales F (2005) Virulence attenuation in *Salmonella enterica rcsC* mutants with constitutive activation of the Rcs system. Microbiol 151(Pt 2):579–588
- Gervais FG, Drapeau GR (1992) Identification, cloning, and characterization of *rcsF*, a new regulator gene for exopolysaccharide synthesis that suppresses the division mutation *ftsZ84* in *Escherichia coli* K-12. J Bacteriol 174:8016–8022
- Gervais FG, Phoenix P, Drapeau GR (1992) The *rcsB* gene, a positive regulator of colonic acid biosynthesis in *Escherichia coli*, is also an activator of *ftsZ* expression. J Bacteriol 174:3964–3971
- Gibbs KA, Urbanowski ML, Greenberg EP (2008) Genetic determinants of self-identity and social recognition in bacteria. Science 321(5886):256–259
- Gottesman S, Trisler P, Torres-Cabassa AS (1985) Regulation of capsular polysaccharide synthesis in *Escherichia coli* K12: characterization of three regulatory genes. J Bacteriol 162:1111–1119
- Gygi D, Bailey MJ, Allison C, Hughes C (1995) Requirement for FlhA in flagella assembly and swarm cell differentiation by *Proteus mirabilis*. Mol Microbiol 15:761–769
- Hagiwara D, Sugiura M, Oshima T, Mori H, Aiba H, Yamashino T, Mizuno T (2003) Genome-wide analyses revealing a signaling network of the RcsC-YojN-RcsB phosphorelay system in *Escherichia coli*. J Bacteriol 185(19):5735–5746
- Hay NA, Tipper DJ, Gygi D, Hughes C (1999) A Novel Membrane Protein Influencing Cell Shape and Multicellular Swarming of *Proteus mirabilis*. J Bacteriol 181(7):2008–2016
- Hinchliffe SJ, Howard SL, Huang YH, Clarke DJ, Wren BW (2008) The importance of the Rcs phosphorelay in the survival and pathogenesis of the enteropathogenic yersiniae. Microbiol 154(4):1117–1131
- Hoening JFM (1965) Development of flagella by *Proteus mirabilis*. J Gen Microbiol 40:29–42
- Howery KE, Clemmer KM, Simsek E, Kim M, Rather PN (2015) Regulation of the Min cell division inhibition system by the Rcs phosphorelay in *Proteus mirabilis*. J Bacteriol 197(15):2499–2507
- Jackson DW, Suzuki K, Oakford L, Simecka JW, Hart ME, Romeo T (2002) Biofilm formation and dispersal under the influence of the global regulator CsrA of *Escherichia coli*. J Bacteriol 184(1):290–301
- Jacobsen SM, Stickler DJ, Mobley HL, Shirtliff ME (2008) Complicated catheter-associated urinary tract infections due to *Escherichia coli* and *Proteus mirabilis*. Clin Microbiol Rev 21(1):26–59
- Jander G, Rahme LG, Ausubel FM (2000) Positive correlation between virulence of *Pseudomonas aeruginosa* mutants in mice and insects. J Bacteriol 182:3843–3845
- Jansen AM, Lockett CV, Johnson DE, Mobley HL (2003) Visualization of *Proteus mirabilis* morphotypes in the urinary tract: the elongated swarmer cell is rarely observed in ascending urinary tract infection. Infect Immun 71:3607–3950
- Jansen AM, Lockett V, Johnson DE, Mobley HLT (2004) Mannose-resistant proteus-like fimbriae are produced by most *Proteus mirabilis* strains infecting the urinary tract, dictate the in vivo localization of bacteria, and contribute to biofilm formation. Infect Immun 72:7294–7305
- Jones BV, Young R, Mahenthalingam E, Stickler DJ (2004) Ultrastructure of *Proteus mirabilis* swarmer cell rafts and the role of swarming in catheter-associated urinary tract infections. Infect Immun 72:3941–3950
- Kovács AT (2016) Bacterial differentiation via the gradual activation of global regulators. Curr Genet 62:125–128
- Lehti TA, Heikkinen J, Korhonen TK, Westerlund-Wikström B (2012) The response regulator RcsB activates expression of Mat fimbriae in meningitic *Escherichia coli*. J Bacteriol 194(13):3475–3485
- Li X, Johnson DE, Mobley HLT (1999) Requirement of MrpH for mannose-resistant *Proteus*-like fimbriae-mediated hemagglutination by *Proteus mirabilis*. Infect Immun 67(6):2822–2833
- Li X, Rasko DA, Lockett CV, Johnson DE, Mobley HLT (2001) Repression of bacterial motility by a novel fimbrial gene product. EMBO J 20:4854–4862
- Liaw SJ, Lia HC, Ho SW, Luh KT, Wang WB (2001) Characterisation of *p*-nitrophenylglycerol-resistant *Proteus mirabilis* super-swarming mutants. J Med Microbiol 50(12):1039–1048
- Liaw SJ, Lai HC, Wang WB (2004) Modulation of swarming and virulence by fatty acids through the RsbA protein in *Proteus mirabilis*. Infect Immun 72(12):6836–6845
- Lower BH, Yongsunthorn R, Vellano FP, Lower SK (2005) Simultaneous force and fluorescence measurements of a protein that forms a bond between a living bacterium and a solid surface. J Bacteriol 187(6):2127–2137

- Majdalani N, Hernandez D, Gottesman S (2002) Regulation and mode of action of the second small RNA activator of RpoS translation. *RprA Mol Microbiol* 46:813–826
- Majdalani N, Heck M, Stout V, Gottesman S (2005) Role of RcsF in signaling to the Rcs phosphorelay pathway in *Escherichia coli*. *J Bacteriol* 187:6770–6778
- Massad G, Lockatell CV, Johnson DE, Mobley HLT (1994) *Proteus mirabilis* fimbriae: construction of an isogenic *pmfA* mutant and analysis of virulence in a CBA mouse model of ascending urinary infection. *Infect Immun* 62:536–542
- Matsukawa M, Kunishima Y, Takahashi S, Takeyama K, Tsukamoto T (2005) Bacterial colonization on intraluminal surface of urethral catheter. *Urology* 65:440–444
- Mobley HL, Chippendale GR, Tenney JH, Mayrer AR, Crisp LJ, Penner JL, Warren JW (1988) MR/K hemagglutination of *Providencia stuartii* correlates with adherence to catheters and with persistence in catheter-associated bacteriuria. *J Infect Dis* 157(2):264–271
- Mobley HL, Chippendale GR, Swihart KG, Welch RA (1991) Cytotoxicity of the HpmA hemolysin and urease of *Proteus mirabilis* and *Proteus vulgaris* against cultured human renal proximal tubular epithelial cells. *Infect Immun* 59:2036–2042
- Mobley HL, Belas R, Lockatell V, Chippendale G, Trifillis AL, Johnson DE, Warren JW (1996) Construction of a flagellum-negative mutant of *Proteus mirabilis*: effect on internalization by human renal epithelial cells and virulence in a mouse model of ascending urinary tract infection. *Infect Immun* 64(12):5332–5340
- Morgenstein RM, Clemmer KM, Rather PN (2010) Loss of the *waalO*-antigen ligase prevents surface activation of the flagellar gene cascade in *Proteus mirabilis*. *J Bacteriol* 192(12):3213–3221
- Mrázek J, Xie S (2006) Pattern locator: a new tool for finding local sequence patterns in genomic DNA sequences. *Bioinformatics* 22:3099–3100
- Murherjee K, Altincicek B, Hain T, Domann E, Vilcinskas A, Chakraborty T (2010) *Galleria mellonella* as a model system for studying *Listeria* pathogenesis. *Appl Environ Microbiol* 76:310–317
- O'Hara CM, Brenner FW, Miller JM (2000) Classification, identification, and clinical significance of *Proteus*, *Providencia*, and *Morganella*. *Clin Microbiol Rev* 13(4):534–546
- Pearson MM, Mobley HLT (2008) Repression of motility during fimbrial gene expression: identification of 14 *mrpJ* gene paralogues in *Proteus mirabilis*. *Mol Microbiol* 69:548–558
- Pearson MM, Sebahia M, Churcher C, Quail MA, Seshasayee AS, Luscombe NM, Abdellah Z, Arrosmith C, Atkin B, Chillingworth T, Hauser H, Jagels K, Moule S, Mungall K, Norbertczak H, Rabinowitsch E, Walker D, Whithead S, Thomson NR, Rather PN, Parkhill J, Mobley HL (2008) Complete genome sequence of uropathogenic *Proteus mirabilis*, a master of both adherence and motility. *J Bacteriol* 190(11):4027–4037
- Pearson MM, Rasko DA, Smith SN, Mobley HLT (2010) Transcriptome of swarming *Proteus mirabilis*. *Infect Immun* 78:2834–2845
- Pearson MM, Yep A, Smith SN, Mobley HL (2011) Transcriptome of *Proteus mirabilis* in the murine urinary tract: virulence and nitrogen assimilation gene expression. *Infect Immun* 79(7):2619–2631
- Pellegrino R, Scavone P, Umpiérrez A, Maskell DJ, Zunino P (2013) *Proteus mirabilis* uropathelial cell adhesin (UCA) fimbria plays a role in the colonization of the urinary tract. *Pathog Dis* 67(2):104–107
- Phan V, Belas R, Gilmore BF, Ceri H (2008) ZapA, a virulence factor in a rat model of *Proteus mirabilis*-induced acute and chronic prostatitis. *Infect Immun* 76(11):4859–4864
- Pichoff S, Lutkenhaus J (2005) Tethering the Z ring to the membrane through a conserved membrane targeting sequence in FtsA. *Mol Microbiol* 55(6):1722–1734
- Pristovsek P, Sengupta K, Lohr F, Schafer B, von Trebra MW, Ruterjans H, Bernhard F (2003) Structural analysis of the DNA-binding domain of the *Erwinia amylovora* RcsB protein and its interaction with the RcsAB box. *J Biol Chem* 278:17752–17759
- Ramarao N, Nielsen-Leroux C, Lereclus D (2012) The insect *Galleria mellonella* as a powerful infection model to investigate bacterial pathogenesis. *J Visual Exp* 11(70):e4392
- Rauprich O, Matsushita M, Weijer CJ, Siegert F, Esipov SE, Shapiro JA (1996) Periodic phenomena in *Proteus mirabilis* swarm colony development. *J Bacteriol* 178:6525–6538
- Roberts JA, Fussell EN, Kaack MB (1990) Bacterial adherence to urethral catheters. *J Urol* 144:264–269
- Rocha S, Elias W, Cianciarullo A, Menezes M, Nara J, Piazza R, Silva M, Moreira C, Pelayo J (2007) Aggregative adherence of uropathogenic *Proteus mirabilis* to cultured epithelial cells. *FEMS Immun Med Microbiol* 51(2):319–326
- Sabbuba N, Hughes G, Stickler DJ (2002) The migration of *Proteus mirabilis* and other urinary tract pathogens over Foley catheters. *BJU Int* 89(1):55–60
- Schwan WR, Shibata S, Aizawa S, Wolfe AJ (2007) The two-component response regulator RcsB regulates type 1 piliation in *Escherichia coli*. *J Bacteriol* 189(19):7159–7163
- Seed KD, Dennis JJ (2008) Development of *Galleria mellonella* as an alternative infection model for the *Burkholderia cepacia* complex. *Infect Immun* 76:1267–1275
- Senior BW, Loomes LM, Kerr MA (1991) The production and activity in vivo of *Proteus mirabilis* IgA protease in infections of the urinary tract. *J Med Microbiol* 35(4):203–207
- Stevenson LG, Rather PN (2006) A novel gene involved in regulating the flagellar gene cascade in *Proteus mirabilis*. *J Bacteriol* 188:7830–7839
- Stickler DJ, Lear JC, Morris NS, Macleod SM, Downer A, Cadd DH, Feast WJ (2006) Observations on the adherence of *Proteus mirabilis* onto polymer surfaces. *J Appl Microbiol* 100:1028–1033
- Stout V, Gottesman S (1990) RcsB and RcsC: a two-component regulator of capsule synthesis in *Escherichia coli*. *J Bacteriol* 172:659–669
- Stout V, Torres-Cabassa A, Maurizi MR, Gutnick D, Gottesman S (1991) RcsA, an unstable positive regulator of capsular polysaccharide synthesis. *J Bacteriol* 173:1738–1747
- Sturgill G, Rather PN (2004) Evidence that putrescine acts as an extracellular signal required for swarming in *Proteus mirabilis*. *Mol Microbiol* 51:437–446
- Swihart KG, Welch RA (1990) Cytotoxic activity of the *Proteus* hemolysin HpmA. *Infect Immun* 58(6):1861–1869
- Takeda S, Fujisawa Y, Matsubara M, Aiba H, Mizuno T (2001) A novel feature of the multistep phosphorelay in *Escherichia coli*: a revised model of the RcsC → YojN → RcsB signalling pathway implicated in capsular synthesis and swarming behavior. *Mol Microbiol* 40:440–450
- Walker KE, Moghaddame-Jafari S, Lockatell CV, Johnson D, Belas R (1999) ZapA, the IgA-degrading metalloprotease of *Proteus mirabilis*, is a virulence factor expressed specifically in swarmer cells. *Mol Microbiol* 32(4):825–836
- Wang Q, Zhao Y, McClelland M, Harshey RM (2007) The RcsCDB signaling system and swarming motility in *Salmonella enterica* serovar typhimurium: dual regulation of flagellar and SPI-2 virulence genes. *J Bacteriol* 189(23):8447–8457
- Wang WB, Chen IC, Jiang SS, Chen HR, Hsu CY, Hseuh PR, Hsu WB, Liaw SJ (2008) Role of RppA in the regulation of polymyxin B susceptibility, swarming and virulence factor expression in *Proteus mirabilis*. *Infect Immun* 76:2051–2062
- Ward JE, Lutkenhaus J (1985) Overproduction of FtsZ induces mini-cell formation in *E. coli*. *Cell* 42:941–949

- Wehland M, Bernhard F (2000) The RcsAB box. Characterization of a new operator essential for the regulation of exopolysaccharide biosynthesis in enteric bacteria. *J Biol Chem* 275(10):7013–7020
- Wenren LM, Sullivan NL, Cardarelli L, Septer AN, Gibbs KA (2013) Two independent pathways for self-recognition in *Proteus mirabilis* are linked by type VI-dependent export. *Mbio* 4(4):e374–e413
- Yakubu DE, Old DC, Senior BW (1989) The haemagglutinins and fimbriae of *Proteus penneri*. *J Med Microbiol* 30(4):279–284
- Zunino P, Piccini C, Legnani-Fajardo C (1994) Flagellate and non-flagellate *Proteus mirabilis* in the development of experimental urinary tract infection. *Microb Pathog* 16:379–385
- Zunino P, Geymonat L, Allen AG, Preston A, Sosa V, Maskell DJ (2001) New aspects of the role of MR/P fimbriae in *Proteus mirabilis* urinary tract infection. *FEMS Immunol Med Microbiol* 31:113–120
- Zunino P, Sosa V, Allen AG, Preston A, Schlapp G, Maskell DJ (2003) *Proteus mirabilis* fimbriae (PMF) are important for both bladder and kidney colonization in mice. *Microbiol* 149(11):3231–3237